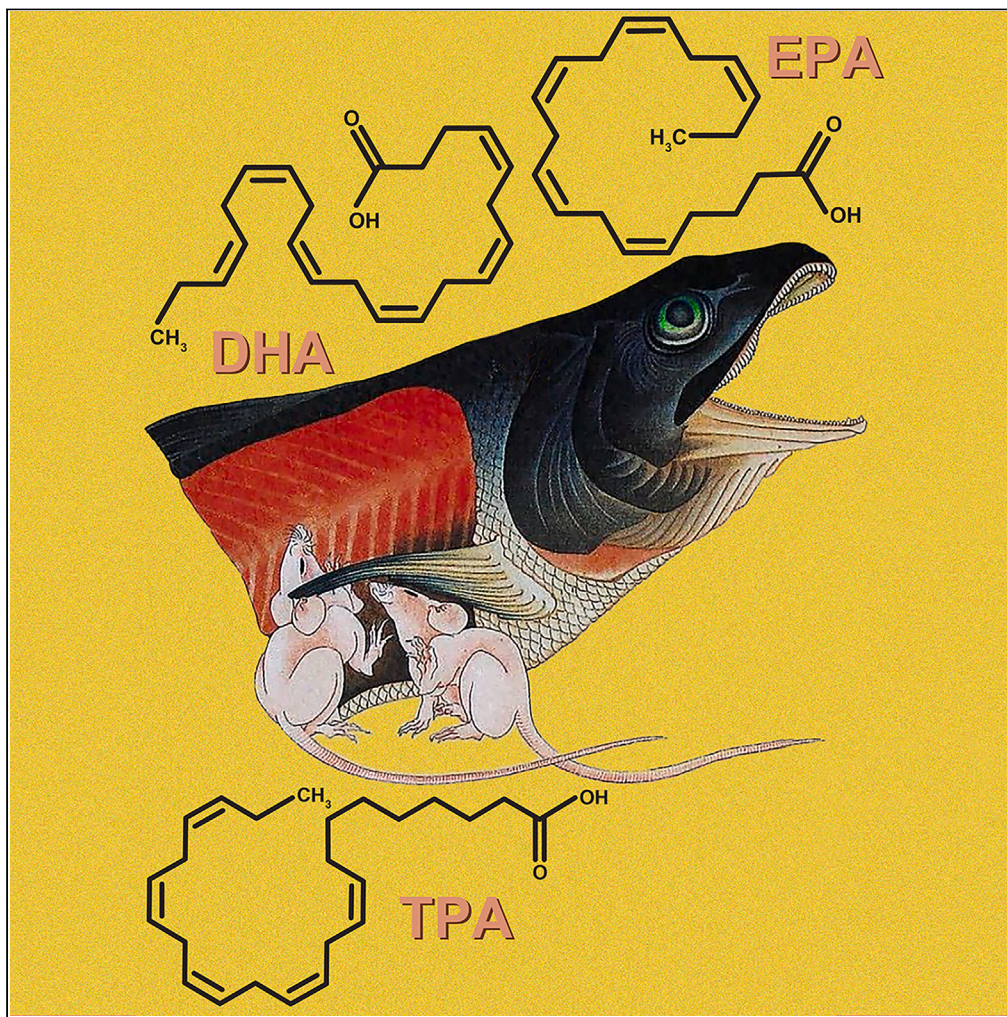


## Article

# Dietary fish oil enriched in very-long-chain polyunsaturated fatty acid reduces cardiometabolic risk factors and improves retinal function



Zhi-Hong Yang,  
Aruna Gorusupudi,  
Todd A. Lydic, ...  
Anand Swaroop,  
Paul S. Bernstein,  
Alan T. Remaley

paul.bernstein@hsc.utah.edu  
(P.S.B.)  
aremaley1@nhlbi.nih.gov  
(A.T.R.)

**Highlights**  
Dietary C24-28-rich VLCPUFAs concentrated from fish oil are bioavailable in mice

Dietary VLCPUFAs are incorporated into the liver, brain, and eyes

VLCPUFA supplement improves cardiometabolic risk factors and retinal function

VLCPUFAs trigger PPAR activation and modulate hepatic gene expression profile

Yang et al., iScience 26, 108411  
December 15, 2023 © 2023  
<https://doi.org/10.1016/j.isci.2023.108411>

## Article

# Dietary fish oil enriched in very-long-chain polyunsaturated fatty acid reduces cardiometabolic risk factors and improves retinal function

Zhi-Hong Yang,<sup>1,8</sup> Aruna Gorusupudi,<sup>2,8</sup> Todd A. Lydic,<sup>3</sup> Anupam K. Mondal,<sup>4</sup> Seizo Sato,<sup>5</sup> Iao Yamazaki,<sup>5</sup> Hideaki Yamaguchi,<sup>5</sup> Jingrong Tang,<sup>1</sup> Krishna Vamsi Rojulpote,<sup>1</sup> Anna B. Lin,<sup>3</sup> Hannah Decot,<sup>3</sup> Hannah Koch,<sup>3</sup> Daniel C. Brock,<sup>4</sup> Ranganathan Arunkumar,<sup>2</sup> Zhen-Dan Shi,<sup>6</sup> Zu-Xi Yu,<sup>7</sup> Milton Pryor,<sup>1</sup> Julia F. Kun,<sup>1</sup> Rolf E. Swenson,<sup>6</sup> Anand Swaroop,<sup>4</sup> Paul S. Bernstein,<sup>2,\*</sup> and Alan T. Remaley<sup>1,9,\*</sup>

## SUMMARY

**Very-long-chain polyunsaturated fatty acids (VLCPUFAs; C24-38) constitute a unique class of PUFA that have important biological roles, but the lack of a suitable dietary source has limited research in this field. We produced an n-3 C24-28-rich VLCPUFA-oil concentrated from fish oil to study its bioavailability and physiological functions in C57BL/6J mice. The serum and retinal C24:5 levels increased significantly compared to control after a single-dose gavage, and VLCPUFAs were incorporated into the liver, brain, and eyes after 8-week supplementation. Dietary VLCPUFAs resulted in favorable cardiometabolic changes, and improved electroretinography responses and visual performance. VLCPUFA supplementation changed the expression of genes involved in PPAR signaling pathways. Further *in vitro* studies demonstrated that the VLCPUFA-oil and chemically synthesized C24:5 are potent agonists for PPARs. The multiple potential beneficial effects of fish oil-derived VLCPUFAs on cardiometabolic risk and eye health in mice support future efforts to develop VLCPUFA-oil into a supplemental therapy.**

## INTRODUCTION

Numerous animal and human studies have shown that diets enriched in oily fish that contain n-3 polyunsaturated fatty acids (PUFAs), such as eicosapentaenoic acid (EPA; 20:5 n-3) and docosahexaenoic acid (DHA; 22:6 n-3), are associated with a lower risk for cardiovascular disease (CVD), as well as age-related macular degeneration (AMD). The mechanisms of these associations are not clearly known but have been proposed to involve potent anti-inflammatory, anti-angiogenic and neuroprotective activities of n-3 PUFA.<sup>1,2</sup> Supplementation with EPA+DHA, however, did not show benefit in delaying AMD progression in several large randomized controlled trials.<sup>3,4</sup>

In addition to n-3 PUFA, marine fish oils contain small amounts of n-3 very-long-chain PUFAs (VLCPUFAs) with greater than 22 carbon atoms, but these are typically lost during the manufacturing of fish oil supplements enriched in EPA and DHA. VLCPUFAs (C24-C38) are mostly present in certain specialized tissues, such as the retina, brain, and testis, where they are synthesized through a series of elongation steps involving ELOVL (elongation of very-long-chain fatty acids) enzymes, such as ELOVL2 and ELOVL4.<sup>5</sup> There is growing evidence of the physiologic importance of VLCPUFAs in maintaining optimal eye health and function.<sup>6,7</sup> A significant decrease in retinal C24-C34 VLCPUFAs has been described during aging, particularly in AMD.<sup>8</sup> Notably, mutations in the *ELOVL4* gene result in the retinal depletion of VLCPUFAs, causing Stargardt-like macular dystrophy (Type 3), which leads to progressive vision loss and blindness.<sup>7</sup> Decreased levels of VLCPUFAs may also lead to decreased spermatogenesis<sup>9</sup> and result in spinocerebellar ataxia.<sup>10</sup>

A recent short-term feeding study reported the retinal incorporation of chemically synthesized 32:6 n-3, a VLCPUFA product of ELOVL4, with concomitant improved retinal function in wild-type and *Elovl4* conditional knockout mice.<sup>11</sup> Until now, however, no study has examined

<sup>1</sup>Lipoprotein Metabolism Section, Translational Vascular Medicine Branch, National Heart, Lung and Blood Institute (NHLBI), National Institutes of Health (NIH), Bethesda, MD 20892, USA

<sup>2</sup>Department of Ophthalmology and Visual Sciences, John A. Moran Eye Center, Salt Lake City, UT 84132, USA

<sup>3</sup>Department of Physiology, Collaborative Mass Spectrometry Core, Michigan State University, East Lansing, MI 48824, USA

<sup>4</sup>Neurobiology, Neurodegeneration and Repair Laboratory, National Eye Institute, NIH, Bethesda, MD 20892, USA

<sup>5</sup>Central Research Laboratory, Nissui Corporation, 1-32-3 Nanakuni, Hachioji, Tokyo 192-0991, Japan

<sup>6</sup>Chemistry and Synthesis Center, NHLBI, NIH, Bethesda, MD 20892, USA

<sup>7</sup>Pathology Core, NHLBI, NIH, Bethesda, MD 20892, USA

<sup>8</sup>These authors contributed equally

<sup>9</sup>Lead contact

\*Correspondence: paul.bernstein@hsc.utah.edu (P.S.B.), aremaley1@nhlbi.nih.gov (A.T.R.)

<https://doi.org/10.1016/j.isci.2023.108411>



the potential benefits of shorter-chain VLCPUFAs, mainly the product of ELOVL2, for retinal health and other health conditions. ELOVL2 in the n-3 PUFA pathway is responsible for the conversion of docosapentaenoic acid (DPA; 22:5 n-3) to tetracosapentaenoic acid (TPA; 24:5 n-3), a direct precursor of DHA and longer-chain VLCPUFAs. Age-related methylation of the *ELOVL2* gene has been identified as an epigenetic marker of aging.<sup>12</sup> Retinal ELOVL2 levels and visual function decline in older mice, and even early vision loss have also been observed in *Elovl2*-mutant mice with reduced retinal 24:5 n-3 levels.<sup>13</sup> However, the roles of shorter-chain VLCPUFAs remain largely unknown. It is not clear if supplementation of ELOVL-derived VLCPUFAs could slow or reverse the AMD progression. Recently, N32 and N34 elovanoids, VLCPUFA-derived bioactive mediators, were described and shown to have beneficial effects on viability and integrity of photoreceptor cells and retinal pigment epithelium cells.<sup>14</sup> In addition, we hypothesize that n-3 VLCPUFAs may exert beneficial effects against CVD like EPA and DHA through similar mechanisms, such as triglyceride-lowering, enhancement of endothelial function, and secretion of anti-inflammatory lipid mediators.<sup>1</sup>

Therefore, we predict that dietary supplementation of ELOVL2-derived VLCPUFAs would bypass the first elongation step (ELOVL2) in the production of VLCPUFAs and provide a novel approach for treating AMD and reduce CVD risk factors. To test this hypothesis, we developed a C24-28-rich VLCPUFA-oil concentrated from fish oil and used it in dietary studies of mice to first examine its safety, bioavailability, metabolism, and potential physiological functions. Fish oils are already the most commonly used nonvitamin/nonmineral dietary supplements, and our findings could lead to further improvements in the formulation of fish oil supplements for eye and cardiovascular health.

## RESULTS

### Dietary VLCPUFA supplementation is safe

C57BL/6J mice starting at 9-month of age were fed an AIN-93G diet (control; 70 g of soybean oil/kg diet) supplemented with either of two doses of n-3 VLCPUFA-fish oil concentrate: 1% (10 g of soybean oil/kg diet was replaced by VLCPUFA-oil) or 5% (50 g of soybean oil/kg diet was replaced by VLCPUFA-oil). The new fish oil supplement contained over 40% (w/w) VLCPUFAs with carbon chain lengths between C24 and C28 and was particularly enriched in 24:5 n-3 (28.5%, w/w) (Table S1). Part of the soybean oil in the control diet was replaced with VLCPUFA oil so that all the diets contained the same amount of total fat and were isocaloric (3.8 kcal/g diet). Compared to mice fed the control chow diet, there were no differences in the general appearance or behavior of the mice fed the VLCPUFA supplement. VLCPUFA supplementation did not cause significant changes in body weight or any apparent adverse changes in plasma chemistry tests compared to control (Table S2). Histologic analysis of the liver, kidney, spleen, heart, skeletal muscle, small intestine, brain, and testis also showed no changes due to VLCPUFA supplementation after the 8-week feeding period (Figures S3–S11).

### Dietary VLCPUFAs are bioavailable and incorporated into target tissues

In a single-dose oral gavage study, peak serum concentrations of the three main n-3 VLCPUFA-oil components, i.e., 24:5, 26:6, and 28:8, were observed at 2 h after dosing ( $p < 0.05$  vs. baseline) (Figure 1A). In the retina, 24:5 peaked at 8 h, yet no retinal enrichment was observed for 26:6 or 28:8. In the case of 24:6, a minor component of the VLCPUFA-oil, reached the maximum concentration at 2 h in serum and at 8 h in the retina. No other serum or retinal changes for the other measured fatty acids were observed over time, except for a small increase in retinal 28:4 levels at 24 h after dosing ( $p < 0.05$  vs. baseline). Based on the rapid absorption of orally administered fish oil VLCPUFA concentrate, which agrees with previous observations where chemically synthesized C32:6 was used,<sup>11</sup> we euthanized mice following a light fasting (5 h) in the 8-week dietary study to capture the change in plasma levels of VLCPUFAs. Mice on VLCPUFA supplementation for 8 weeks showed higher levels of 24:5, 26:6, and 28:8 in the plasma, liver, brain, and eyes compared with control diet (Figure 1B and Table S3). Increased tissue levels of 26:5 were also detected in the brain and eyes, possibly from elongation of the dietary 24:5. In contrast, liver levels of 24:6, 26:5, and 28:5, for which 24:5 is also a precursor, were all reduced in a dose-dependent manner after VLCPUFA supplementation. For n-3 PUFAs with carbon chain lengths less than 24, dietary VLCPUFA-oil supplementation did not change plasma EPA and DHA levels, but EPA, DHA, and DPA increased in the liver, brain, and eyes. Dietary VLCPUFA supplementation also caused an overall decrease in n-6 PUFA in the plasma, liver, brain and eyes.

In the multi-organ lipidomic analysis, 560–800 individual lipid signals covering phospholipid (PL), sphingolipid (SL), glycerolipid (GL), sterol lipid (ST), and free fatty acid (FFA) classes were identified by high-resolution accurate-mass (HRAM) mass spectrometers (MS) and MS/MS analysis. The amount of VLCPUFAs incorporated into the major lipid classes varied across different tissues. The dietary VLCPUFA supplement significantly increased plasma total VLCPUFAs detected in GL, ST, and FFA, enhanced hepatic VLCPUFAs in SL, and increased eye VLCPUFAs in SL, GL, and FFA compared with the control ( $p < 0.05$ ) (Figure 1C). The PLS-DA score plot and heatmap of lipid metabolite abundance in the plasma, liver, brain, and eyes clearly showed that dietary VLCPUFAs significantly remodeled lipid species in both male and female mice, in a dose-dependent manner (Figure S12). It also caused a modest change in the percent of total lipid class composition for the plasma, liver, and eyes (Figure 1D and Table S4). Notably, it decreased GL levels in liver and eyes compared with control, mostly due to a decrease in triglyceride levels ( $p < 0.05$ ).

### Dietary VLCPUFAs improve visual function

To evaluate retinal function, we performed an electroretinogram (ERG) analysis. The 2-week repeated gavage feeding study of VLCPUFAs in both male and female mice resulted in consistent increases in photopic a- ( $p < 0.05$  at -5, 0, 5, 10, and 15 dB) and b-wave ( $p < 0.05$  at 0 and 5 dB,  $p = 0.08$  at 10 dB) amplitudes compared with control mice (Figures 2A and S13). No significant change was observed in the scotopic a- and b-wave

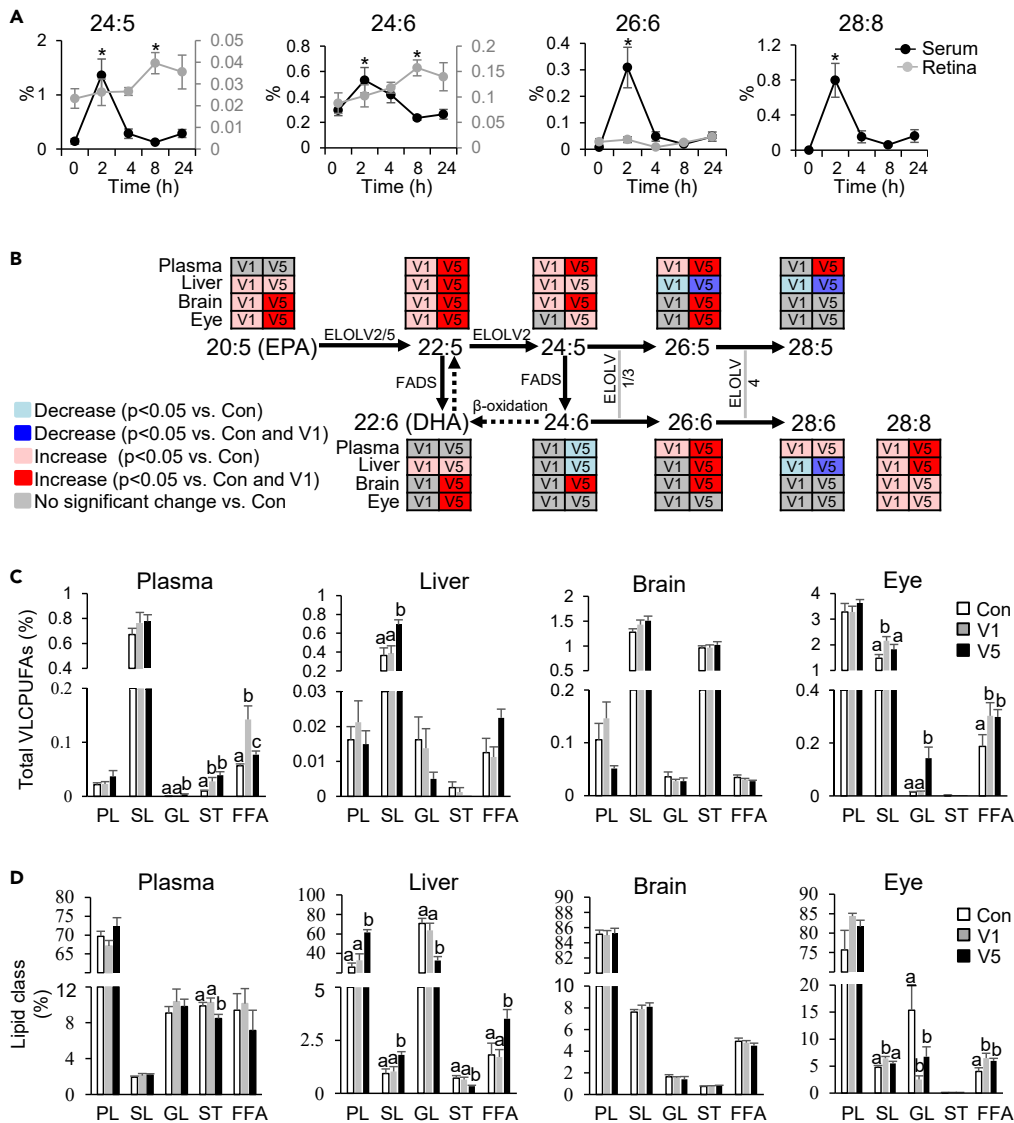


**Figure 1. Dietary VLCPUFAs are bioavailable and incorporated into target tissues**

(A) Serum and retinal levels of 24:5 n-3, 24:6 n-3, 26:6 n-3, and 28:8 n-3 at 0, 2, 4, 8, and 24 h in C57BL/6J mice after a single-dose oral gavage of VLCPUFA-oil (250 mg/kg body weight). Data are represented as mean  $\pm$  SEM ( $n = 5$  per time point). \* $p < 0.05$  vs. 0 h.

(B) Changes in major n-3 PUFA/VLCPUFAs in plasma, liver, brain and eyes in C57BL/6J mice on chow diet supplemented with 1% or 5% (w/w) VLCPUFA-oil, or none (control) for 8 weeks. Decreased ( $p < 0.05$ ), increased ( $p < 0.05$ ), and unchanged fatty acids in 1% and 5% VLCPUFA groups compared with control were colored by blue, red, and gray, respectively ( $n = 8$ ).

(C) Total VLCPUFAs composition (%) in PL, SL, GL, ST, and FFA in the plasma, liver, brain and eyes in C57BL/6J mice on chow diet supplemented with 1% or 5% (w/w) VLCPUFA-oil, or none (control) for 8 weeks. Data are represented as mean  $\pm$  SEM ( $n = 8$ ). <sup>a-c</sup>Means within a column without a common superscript letter differ ( $p < 0.05$ ).

(D) Relative abundance (%) of PL, SL, GL, ST, and FFA in plasma, liver, and eyes in C57BL/6J mice on chow diet supplemented with 1% or 5% (w/w) VLCPUFA-oil, or none (control) for 8 weeks. Data are represented as mean  $\pm$  SEM ( $n = 8$ ). <sup>a-c</sup>Means within a column without a common superscript letter differ ( $p < 0.05$ ). Con: control; V1: 1% VLCPUFA-oil; V5: 5% VLCPUFA-oil; PL: phospholipids; SL: sphingolipids; GL: glycerolipids; ST: sterol lipids; FFA: free fatty acids. See also Figures S12, Table S3 and S4.

responses. VLCPUFAs gavage-fed mice also exhibited increases in photopic ( $p < 0.05$ ) and scotopic ( $p = 0.08$ ) visual acuity compared with control mice (Figures 2B and S13). Finally, scotopic contrast sensitivity also improved after the VLCPUFA treatment ( $p < 0.05$ ) (Figures 2C and S13).

### Dietary VLCPUFAs cause cardiometabolic changes in the plasma and liver

After the 8-week diet intervention study, dietary VLCPUFAs dose-dependently lowered plasma glucose and insulin, as well as the homeostasis model assessment-insulin resistance (HOMA-IR) index in both male and female mice, compared to control chow fed mice ( $p < 0.05$ )

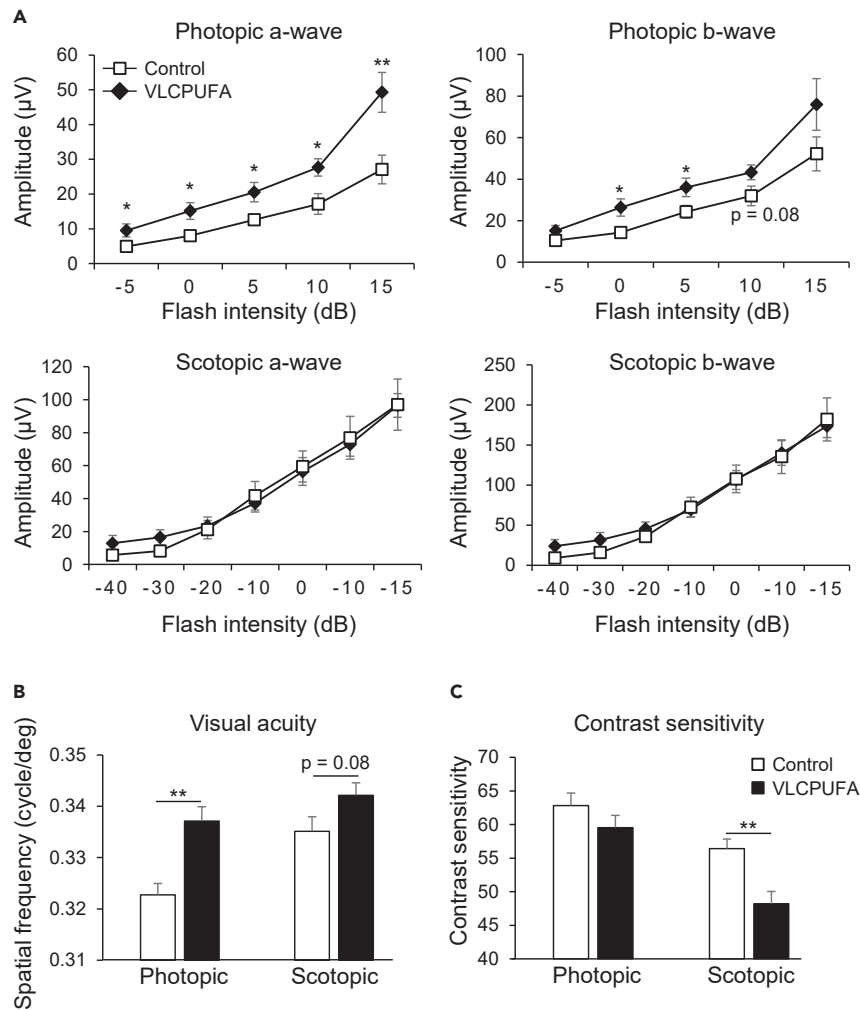


**Figure 2. Dietary VLCPUFAs improve visual function**

(A) Amplitudes of photopic ERG a- and b-waves, and scotopic ERG a- and b-waves plotted versus flash intensity. Data are represented as mean  $\pm$  SEM ( $n = 8$ ). \* $p < 0.05$ , \*\* $p < 0.01$  vs. control.

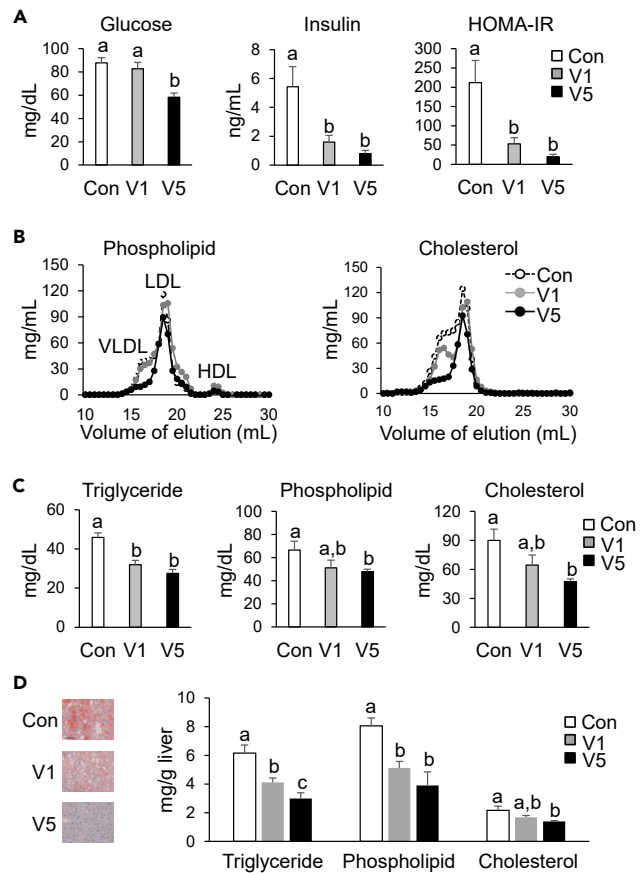
(B) Photopic and scotopic visual acuities. Data are represented as mean  $\pm$  SEM ( $n = 8$ ). \*\* $p < 0.01$  vs. control.

(C) Photopic and scotopic contrast sensitivity. Averaged data were from both eyes of each animal. Data are represented as mean  $\pm$  SEM ( $n = 8$ ). \*\* $p < 0.01$  vs. control. Mice received a daily oral gavage of VLCPUFA-oil (250 mg/kg body weight) or vehicle (control) for 15 consecutive days. See also Figure S13.

(Figures 3A and S14). The VLCPUFA-rich diet also lowered plasma triglycerides, phospholipids, and total cholesterol levels in a dose-dependent manner, corresponding to the observed reduction in the levels of pro-atherogenic very-low-density lipoprotein (VLDL) and low-density lipoprotein (LDL) fractions by fast protein liquid chromatography (FPLC) analysis ( $p < 0.05$ ) (Figures 3B, 3C, and S14). In addition, dietary VLCPUFA-oil showed a dose-dependent effect in lowering hepatic triglycerides and cholesterol in both male and female mice ( $p < 0.05$ ) (Figures 3D and S14). These results were further confirmed with hematoxylin and eosin (H&E) and Oil Red O staining of the liver sections (Figures S3 and S4).

#### Dietary VLCPUFAs alter hepatic transcriptional profile

To further investigate the underlying regulatory mechanism, we generated RNA-seq data from livers of mice on chow and VLCPUFA diets. Principal component analysis (PCA) plots of the 11,339 genes identified by RNA-seq analysis revealed dose-dependent clustering of mice fed a 0%, 1%, or 5% supplemented VLCPUFA diet for 8 weeks (Figure 4A). Differential expression analysis using a dosage-regressed design revealed significant alterations in a total of 261 genes, with 161 genes showing higher and 100 genes showing reduced expression in VLCPUFA-treated livers (Figures 4B and 4C). The top up-regulated genes included *Cyp4a* genes (*Cyp4a10*, *Cyp4a14*, and *Cyp4a31*), *Acot1*, *Slc25c20*, and *Lpl*, whereas the prominently downregulated genes featured *C9* and *C4b*. At higher dosage, dietary VLCPUFAs also upregulated *Pdhb*

**Figure 3. Dietary VLCPUFAs cause cardiometabolic changes in plasma and liver**

(A) Plasma glucose metabolism biomarkers: glucose, insulin, and HOMA-IR levels. Data are represented as mean  $\pm$  SEM ( $n = 8$ ). <sup>a-c</sup>Means within a column without a common superscript letter differ ( $p < 0.05$ ).

(B) Representative plasma phospholipid and cholesterol FPLC profile from plasma samples pooled from 8 mice per group.

(C) Plasma lipid metabolism biomarkers: triglycerides, phospholipid, and total cholesterol levels. Data are represented as mean  $\pm$  SEM ( $n = 8$ ). <sup>a-c</sup>Means within a column without a common superscript letter differ ( $p < 0.05$ ).

(D) Representative images of Oil Red O staining of liver sections and enzymatic measurement of hepatic triglycerides, phospholipid, and cholesterol contents. Data are represented as mean  $\pm$  SEM ( $n = 8$ ). <sup>a-c</sup>Means within a column without a common superscript letter differ ( $p < 0.05$ ). Scale bar represents 100  $\mu$ m. Nine-month-old C57BL/6J mice were fed a chow diet supplemented with 1% or 5% (w/w) VLCPUFA-oil, or none (control) for 8 weeks. Con: control; V1: 1% VLCPUFA-oil; V5: 5% VLCPUFA-oil; HOMA-IR: homeostatic model assessment for insulin resistance; FPLC: fast protein liquid chromatography. See also Figures S3, S4, S14, and Table S2.

and downregulated *Pck*, *Elovl2*, and *Elovl5* (Figures 4D and S15). Our KEGG pathway enrichment analysis demonstrated significant changes in several metabolism-linked processes, including fatty acid metabolism, peroxisome, and peroxisome proliferator-activated receptor (PPAR) signaling pathways (Figures 4E and S15). Differential expression analysis also showed a dose-response effect for many of the identified genes (Figure S15). Based on the observed gene expression changes, we examined the effect of the VLCPUFA-oil used to prepare the mouse chow on PPAR $\alpha$  and PPAR $\gamma$  signaling. PPAR luciferase reporter assays in Chinese hamster ovary (CHO) cells showed that the VLCPUFA-oil dose dependently increased transactivation of both PPAR subtypes ( $p < 0.05$  for 1.6, 5, and 16  $\mu$ g/mL) (Figure 4F). Chemically synthesized 24:5 n-3 (Figures 4G and S2), the most abundant VLCPUFA component in the VLCPUFA-rich fish oil used in the animal studies, also showed agonist activity for PPAR $\alpha$  and PPAR $\gamma$ . In fact, purified 24:5 was more potent than either pure EPA or DHA at 10 and 30  $\mu$ M ( $p < 0.05$ ) (Figure 4H).

## DISCUSSION

Despite growing evidence of the physiologic importance of VLCPUFAs, research on the therapeutic potential of VLCPUFA supplementation has long been hampered by the lack of suitable dietary sources to conduct such studies.<sup>15</sup> Here, we report on the large-scale production of a C24-C28-rich VLCPUFA concentrate made from fish oil and examine its safety, bioavailability, metabolism, and potential roles in retinal function.

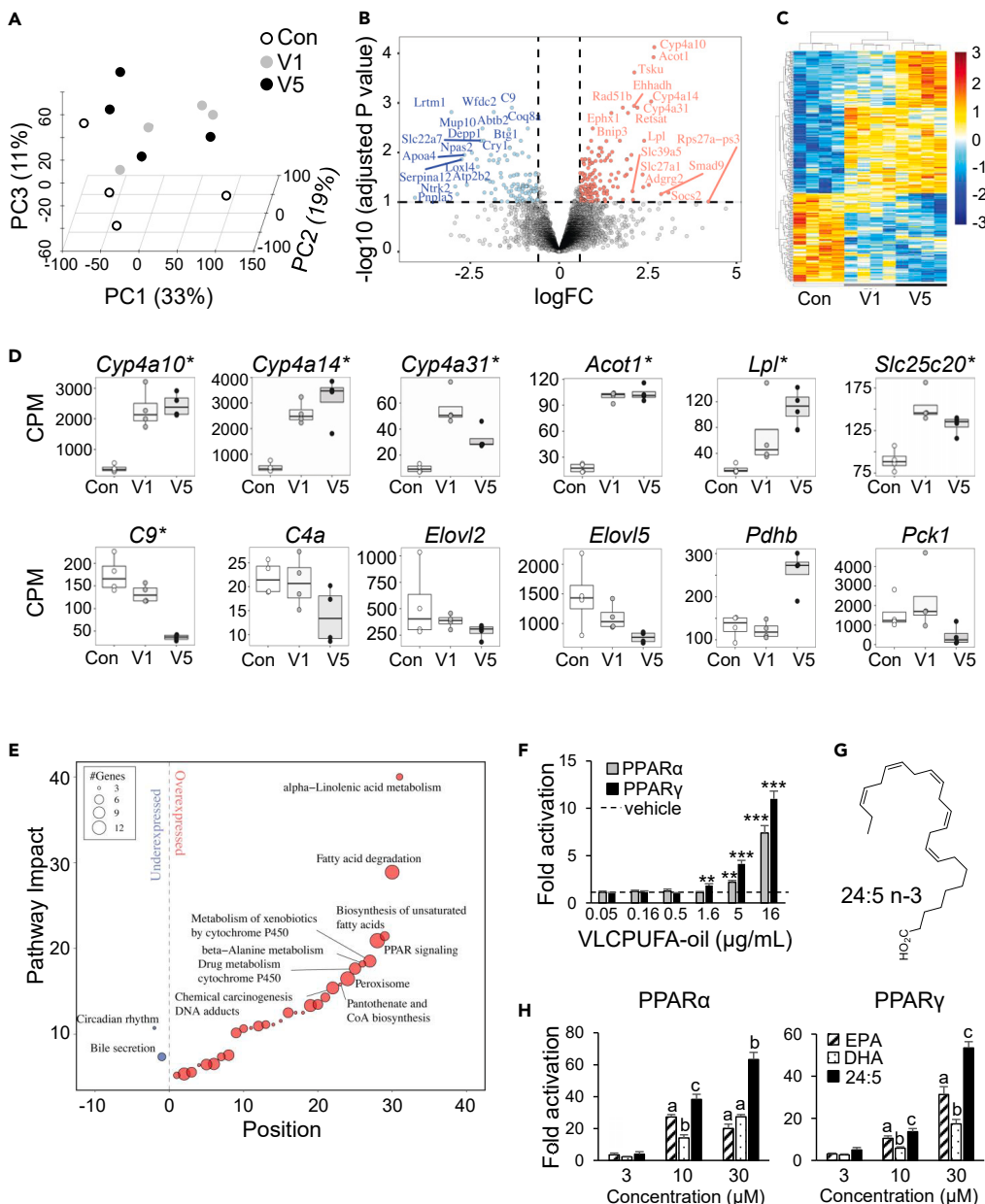


**Figure 4.** Dietary VLCPUFAs alter hepatic transcriptional profile and activates PPARs

(A) 3D-PCA plot showing samples clustering by control (white dots), 1% VLCPUFAs (gray dots), and 5% VLCPUFAs diet (black dots) ( $n = 4$ ).

(B) Differential gene expression summarized in a volcano plot with gene names highlighted for top genes by significance or magnitude.

(C) Heatmap of expression trends of significant differentially expressed genes.

(D) Expression changes among genes involved in glucose and lipid metabolism. \* $p < 0.05$  between the control and VLCPUFA groups.

(E) Pathway enrichment analysis of VLCPUFA-related differential expression. Pathway impact represents percentage of KEGG pathway overlapping over- or under-expressing genes colored by red and blue bubbles, respectively. Nine-month-old C57BL/6J mice were fed a chow diet supplemented with 1% or 5% (w/w) VLCPUFA-oil, or none (control) for 8 weeks.

(F) Fold activation of PPAR $\alpha$  and PPAR $\gamma$  by different dosages of VLCPUFA-oil in CHO cells that have a luciferase reporter gene functionally linked to a PPAR $\alpha$  or PPAR $\gamma$ -response element. Data are represented as mean  $\pm$  SEM ( $n = 3$ ). \*\* $p < 0.01$ , \*\*\* $p < 0.001$  vs. vehicle control ethanol (set to 1.0).

(G) Structure of 24:5 n-3.

(H) Fold activation of PPAR $\alpha$  and PPAR $\gamma$  by chemically synthesized 24:5 n-3 compared with EPA and DHA in CHO cells. Data are represented as mean  $\pm$  SEM ( $n = 3$ ).  $^{\text{a}}$ Means within a column without a common superscript letter differ ( $p < 0.05$ ). PCA: principal component analysis; Con: control; V1: 1% VLCPUFA-oil; V5: 5% VLCPUFA-oil; PPAR: Peroxisome proliferator-activated receptor. See also [Figures S2](#) and [S15](#).

Dietary VLCPUFA-oil showed no adverse effects, using doses comparable with previous animal studies of VLCPUFAs.<sup>11,16</sup> The single-dose oral administration of the VLCPUFA-oil caused a rapid increase in plasma levels of 24:5, followed by increased tissue levels in the retina. Despite the relatively low content of 24:6 in the VLCPUFA-oil, it also increased in the retina, possibly due to conversion of 24:5 by delta-6 desaturase.<sup>17</sup> The content of 26:6 in VLCPUFA-oil was much lower than 24:5, which may explain why retinal levels of 26:6 did not change after a single-dose oral gavage. Neither did retinal levels of 28:8, a unique VLCPUFA species that is almost exclusively found in fish possibly due to dietary transfer from phytoplankton.<sup>18</sup> In the 8-week free feeding study, VLCPUFA supplementation changed overall fatty acid and lipid class compositions in plasma and targeted tissues in a dose-dependent manner compared with control, with non-significant differences between female and male mice. Based on lipid composition changes, there appeared to be some limited elongation of dietary 24:5 to 26:5 in the brain and retina. Conversion to longer-chain VLCPUFA species (C > 28), however, was not observed possibly due to feedback inhibition of ELOVL4. Induction of the cytochrome P450 pathways for the degradation of VLCPUFAs,<sup>19</sup> which we observed in the liver, could also possibly account for the lack of accumulation of longer-chain VLCPUFAs. We also did not see any evidence of longer-chain VLCPUFAs accumulating in the liver, but this was expected because ELOVL4 is mostly expressed in the eyes and brain. We did observe increases in EPA and DHA in the liver, brain, and eyes, which may have occurred by retro-conversion of VLCPUFAs and DPA. Overall, our results confirm the previous studies' findings concerning the bioavailability and tissue incorporation of orally administered VLCPUFAs.<sup>11,16</sup> Until now, most studies on dietary PUFA metabolism have focused on shorter-chain fatty acids (C18-C22), so the detailed metabolism of dietary VLCPUFAs remains largely unknown.<sup>20</sup> Further studies using isotopic labeled VLCPUFAs are needed to better understand their possible interconversion and degradation in various tissues.<sup>21</sup>

Interestingly, of all the tissues tested, dietary VLCPUFAs mostly accumulated in the eyes in the SL, GL, and FFA lipid fractions, suggesting a possible important physiologic role in retinal lipid homeostasis. Furthermore, the rapid uptake by the eyes suggests a possible specific import mechanism for VLCPUFAs. In case of DHA esterified to LysoPC, the major facilitator superfamily domain-containing 2a (MFSD2A) transporter is known to be involved in delivering DHA across the blood-brain barrier.<sup>22,23</sup> In addition, previous studies using labeled cholesterol analogs demonstrated a receptor-mediated mechanism of retinal uptake of circulating lipoproteins, as well as intraretinal lipid transport.<sup>24,25</sup> The accumulation of VLCPUFAs after dietary supplementation and their subsequent remodeling may have contributed to the improved electroretinography (ERG) response and visual performance that we observed in the mice after repeated-dose gavage of VLCPUFA-oil. Previous studies treating mice with DHA and chemically synthesized 32:6 n-3 also showed improved retinal function in normal mice.<sup>11,26</sup> Additional mechanistic studies are needed to determine if VLCPUFAs themselves are directly involved in improving vision by possibly altering membrane structure and fluidity, or by altering synaptic activities.<sup>27,28</sup> Alternatively, it could be a VLCPUFA-derived bioactive metabolite or the retroconversion to EPA and DHA that accounts for the observed improvement in retinal function.<sup>29</sup>

In addition to changes in retinal function, VLCPUFA supplementation had favorable effects on lowering several cardiometabolic risk factors, including plasma glucose and lipids. Both male and female mice had similar beneficial metabolic responses to dietary VLCPUFAs. Fish oil supplements containing EPA and DHA have previously been shown to reduce triglycerides and pro-inflammatory cytokines.<sup>30</sup> Pure EPA has been developed into a drug for the prevention of cardiovascular disease.<sup>31</sup> EPA and DHA are thought to mediate these effects by acting as natural ligands for PPARs that are recognized as molecular sensors of fatty acids and fatty acid derivatives, which regulate the expression of a wide range of genes involved in lipid, glucose, and energy metabolism.<sup>32</sup> The AIN-93 growth diet was used as the control diet in the study. It contains increased fat (70 g/kg diet) compared with AIN-93 maintenance diet (40 g fat/kg diet), which may have contributed to observed hepatic steatosis in mice on the control diet. After the 8-week feeding period, dietary VLCPUFAs dose-dependently decreased hepatic lipid levels compared with control. The VLCPUFAs enriched diet also favorably altered the transcriptional regulation of PPAR target genes known to be involved in glucose and lipid metabolism, such as *Pdhb*, *Pck1*, *Lpl*, *Slc25a20*, *Acot1*, *Cyp4a10*, *Cyp4a14*, and *Cyp4a31*. It also decreased the expression of several complement related genes, which are involved in the pathogenesis of AMD.<sup>33</sup> Our *in vitro* studies established a dose-dependent PPAR $\alpha$  and PPAR $\gamma$  activation by the fish oil-derived VLCPUFA-oil, and the chemically synthesized 24:5 n-3, which was even stronger than the effect by n-3 PUFA EPA and DHA. Activation of PPAR $\alpha$  has been shown to lower lipid levels and inhibit the inflammatory response through interacting with pro-inflammatory transcription factors p65 and c-Jun. PPAR $\gamma$  is mostly involved in the regulation of lipid and glucose homeostasis.<sup>34</sup> Besides their effects in reducing CVD risk, PPAR agonists also have favorable effects in several eye diseases, including AMD, partly through regulating retinal neuroprotection, angiogenesis, and oxidative stress.<sup>35</sup>

In conclusion, dietary fish oil-derived VLCPUFAs were well tolerated in mice and appeared to be sufficiently bioavailable to raise VLCPUFA levels in the plasma, brain, and eyes. We also demonstrate that C24-C28-rich VLCPUFA-oil supplementation improved retinal function in mice and had additional benefits in improving glucose metabolism and in lowering plasma lipids, possibly by altering PPAR signaling. Our findings support future studies for investigating VLCPUFAs as a novel approach for the treatment of AMD and cardiometabolic disease.

### Limitations of the study

Although we provide important new information on the possible therapeutic role of C24-C28-rich VLCPUFA supplementation, further studies in other animal models that better mirror human CVD and AMD will be needed to further evaluate their potential efficacy and safety. Examining the impact of any change in respiratory quotient and other metabolic parameters on mice on the VLCPUFA-enriched diet would be useful. In addition, a more detailed lipidomic analysis of erythrocytes and targeted tissues, such as the liver, retina, and brain, will be needed to better understand exogenous VLCPUFA metabolism. In addition, more detailed studies on the optimum dose and the best formulation will also have to be conducted. It is also unclear from our work if VLCPUFAs themselves or their conversion

to another lipid species is responsible for the observed beneficial changes in cardiometabolic markers, retinal function, and gene transcription; thus, further mechanistic type studies, such as identifying VLCPUFA-derived metabolites and comparing VLCPUFA and regular PUFA diets, are also needed.

## STAR★METHODS

Detailed methods are provided in the online version of this paper and include the following:

- KEY RESOURCES TABLE
- RESOURCE AVAILABILITY
  - Lead contact
  - Materials availability
  - Data and code availability
- EXPERIMENTAL MODEL AND STUDY PARTICIPANT DETAILS
- METHOD DETAILS
  - VLCPUFA concentrate oil derived from fish oil
  - Animals experimental design
  - Biochemical assays
  - Histological analysis
  - LC-MS/MS analysis
  - ERG and visual behavior testing
  - RNA-sequencing analysis
  - Quantitative PCR (qPCR) validation
  - Chemical synthesis of 24:5 n-3
  - In vitro PPARs agonist activity assay
- QUANTIFICATION AND STATISTICAL ANALYSIS

## SUPPLEMENTAL INFORMATION

Supplemental information can be found online at <https://doi.org/10.1016/j.isci.2023.108411>.

## ACKNOWLEDGMENTS

This work was supported by the Intramural Research Program of the National Heart, Lung, and Blood Institute and the Office of the Dietary Supplements (ODS) Research Scholars Program at the National Institutes of Health (NIH). Work performed at the University of Utah was supported by a grant from the Foundation Fighting Blindness; an unrestricted departmental grant from Research to Prevent Blindness; and by grants from NIH (EY34497 and EY14800). Additional support was received from the Intramural Research Program of the National Eye Institute (ZIAEY000450 and ZIAEY00546) to A.S. The authors would like to thank Milton English and Matthew Brooks from the Swaroop laboratory at National Eye Institute for assistance in RNA-seq experiments. The authors acknowledge using the NIH-BioWulf high-performance computing facility for NGS data analysis.

## AUTHOR CONTRIBUTIONS

Conceptualization, Z.-H.Y., P.S.B., and A.T.R.; Methodology, Z.-H.Y., A.G., T.A.L., A.K.M., S.S., I.Y., H.Y., J.T., K.V.R., A.B.L., H.D., H.K., D.C.B., R.A., Z.-D.S., Z.-X.Y., M.P., J.F.K., R.E.S., A.S., P.S.B., and A.T.R.; Investigation, Z.-H.Y., A.G., T.A.L., A.K.M., A.B.L., H.D., H.K., R.A., Z.-D.S., Z.-X.Y., and A.T.R.; Writing – Original draft, Z.-H.Y., A.K.M., Z.-D.S., and A.T.R.; Writing – Review and Editing, Z.-H.Y., A.G., T.A.L., A.K.M., S.S., I.Y., H.Y., J.T., K.V.R., A.B.L., H.D., H.K., D.C.B., R.A., Z.-D.S., Z.-X.Y., M.P., J.F.K., R.E.S., A.S., P.S.B., and A.T.R.; Funding acquisition, Z.-H.Y., A.S., P.S.B., and A.T.R.; Supervision, T.A.L., R.E.S., A.S., P.S.B., and A.R.T.

## DECLARATION OF INTERESTS

Z.-H.Y., A.T.R., J.T., K.V.R., S.S., I.Y., H.Y., National Heart, Lung, and Blood Institute, and Nippon Suisan Kaisha have filed a provisional patent application on the therapeutic effects of fish oil-derived VLCPUFA-oil. Z.-D.S., R.E.S., Z.-H.Y., A.T.R., National Heart, Lung, and Blood Institute has filed a provisional patent application on methods to produce VLCPUFAs.

Received: March 2, 2023

Revised: August 31, 2023

Accepted: November 3, 2023

Published: November 7, 2023

## REFERENCES

- Innes, J.K., and Calder, P.C. (2020). Marine Omega-3 (N-3) Fatty Acids for Cardiovascular Health: An Update for 2020. *Int. J. Mol. Sci.* 21, 1362. <https://doi.org/10.3390/ijms21041362>.
- SanGiovanni, J.P., and Chew, E.Y. (2005). The role of omega-3 long-chain polyunsaturated fatty acids in health and disease of the retina. *Prog. Retin. Eye Res.* 24, 87–138. <https://doi.org/10.1016/j.preteyeres.2004.06.002>.
- Souied, E.H., Delcourt, C., Querques, G., Bassols, A., Merle, B., Zourdani, A., Smith, T., and Benlian, P.; Nutritional AMD Treatment 2 Study Group (2013). Nutritional AMD Treatment 2 Study Group Oral docosahexaenoic acid in the prevention of exudative age-related macular degeneration: the Nutritional AMD Treatment 2 study. *Ophthalmology* 120, 1619–1631. <https://doi.org/10.1016/j.ophtha.2013.01.005>.
- Age-Related Eye Disease Study 2 Research Group (2013). Lutein + zeaxanthin and omega-3 fatty acids for age-related macular degeneration: the Age-Related Eye Disease Study 2 (AREDS2) randomized clinical trial. *JAMA* 309, 2005–2015. <https://doi.org/10.1001/jama.2013.4997>.
- Poulos, A. (1995). Very long chain fatty acids in higher animals—a review. *Lipids* 30, 1–14.
- Liu, A., Lin, Y., Terry, R., Nelson, K., and Bernstein, P.S. (2011). Role of long-chain and very long-chain polyunsaturated fatty acids in macular degenerations and dystrophies. *Clin. Lipidol.* 6, 593–613. <https://doi.org/10.2217/clp.11.41>.
- Yeboah, G.K., Lobanova, E.S., Brush, R.S., and Agbaga, M.P. (2021). Very long chain fatty acid-containing lipids: a decade of novel insights from the study of ELOVL4. *J. Lipid Res.* 62, 100030. <https://doi.org/10.1016/j.jlr.2021.100030>.
- Liu, A., Chang, J., Lin, Y., Shen, Z., and Bernstein, P.S. (2010). Long-chain and very long-chain polyunsaturated fatty acids in ocular aging and age-related macular degeneration. *J. Lipid Res.* 51, 3217–3229. <https://doi.org/10.1194/jlr.M007518>.
- Craig, L.B., Brush, R.S., Sullivan, M.T., Zavy, M.T., Agbaga, M.P., and Anderson, R.E. (2019). Decreased very long chain polyunsaturated fatty acids in sperm correlates with sperm quantity and quality. *J. Assist. Reprod. Genet.* 36, 1379–1385. <https://doi.org/10.1007/s10815-019-01464-3>.
- Gyenning, Y.K., Chauhan, N.K., Tytanic, M., Ea, V., Brush, R.S., and Agbaga, M.P. (2023). ELOVL4 Mutations That Cause Spinocerebellar Ataxia-34 Differentially Alter Very Long Chain Fatty Acid Biosynthesis. *J. Lipid Res.* 64, 100317. <https://doi.org/10.1016/j.jlr.2022.100317>.
- Gorusupudi, A., Rallabandi, R., Li, B., Arunkumar, R., Blount, J.D., Rognon, G.T., Chang, F.Y., Wade, A., Lucas, S., Conboy, J.C., et al. (2021). Retinal bioavailability and functional effects of a synthetic very-long-chain polyunsaturated fatty acid in mice. *Proc. Natl. Acad. Sci. USA* 118, e2017739118. <https://doi.org/10.1073/pnas.2017739118>.
- Garagnani, P., Bacalini, M.G., Pirazzini, C., Gori, D., Giuliani, C., Mari, D., Di Blasio, A.M., Gentilini, D., Vitale, G., Collino, S., et al. (2012). Methylation of ELOVL2 gene as a new epigenetic marker of age. *Aging Cell* 11, 1132–1134. <https://doi.org/10.1111/acel.12005>.
- Chen, D., Chao, D.L., Rocha, L., Kolar, M., Nguyen Huu, V.A., Krawczyk, M., Dasyani, M., Wang, T., Jafari, M., Jabari, M., et al. (2020). The lipid elongation enzyme ELOVL2 is a molecular regulator of aging in the retina. *Aging Cell* 19, e13100. <https://doi.org/10.1111/acel.13100>.
- Bazan, N.G. (2021). Overview of how N32 and N34 elovanoids sustain sight by protecting retinal pigment epithelial cells and photoreceptors. *J. Lipid Res.* 62, 100058. <https://doi.org/10.1194/jlr.TR120001137>.
- Rezanka, T. (1989). Very-long-chain fatty acids from the animal and plant kingdoms. *Prog. Lipid Res.* 28, 147–187. [https://doi.org/10.1016/0163-7827\(89\)90011-8](https://doi.org/10.1016/0163-7827(89)90011-8).
- Torrissen, M., Svensen, H., Stoknes, I., Nilsson, A., Østbye, T.K., Berge, G.M., Bou, M., and Ruyter, B. (2022). Deposition and metabolism of dietary n-3 very-long-chain PUFA in different organs of rat, mouse and Atlantic salmon. *Br. J. Nutr.* 127, 35–54. <https://doi.org/10.1017/S0007114521000817>.
- D'andrea, S., Guillou, H., Jan, S., Catheline, D., Thibault, J.N., Bouriel, M., Rioux, V., and Legrand, P. (2002). The same rat Delta6-desaturase not only acts on 18- but also on 24-carbon fatty acids in very-long-chain polyunsaturated fatty acid biosynthesis. *Biochem. J.* 364 (Pt 1), 49–55. <https://doi.org/10.1042/bj3640049>.
- Mansour, M.P., Frampton, D.M.F., Nichols, P.D., Volkman, J.K., and Blackburn, S.I. (2005). Lipid and fatty acid yield of nine stationary-phase microalgae: Applications and unusual C24–C28 polyunsaturated fatty acids. *J. Appl. Phycol.* 17, 287–300.
- Bishop-Bailey, D., Thomson, S., Askari, A., Faulkner, A., and Wheeler-Jones, C. (2014). Lipid-metabolizing CYPs in the regulation and dysregulation of metabolism. *Annu. Rev. Nutr.* 34, 261–279. <https://doi.org/10.1146/annurev-nutr-071813-105747>.
- Saini, R.K., and Keum, Y.S. (2018). Omega-3 and omega-6 polyunsaturated fatty acids: Dietary sources, metabolism, and significance - A review. *Life Sci.* 203, 255–267. <https://doi.org/10.1016/j.lfs.2018.04.049>.
- Liu, L., Bartke, N., Van Daele, H., Lawrence, P., Qin, X., Park, H.G., Kothapalli, K., Windust, A., Bindels, J., Wang, Z., and Brenna, J.T. (2014). Higher efficacy of dietary DHA provided as a phospholipid than as a triglyceride for brain DHA accretion in neonatal piglets. *J. Lipid Res.* 55, 531–539. <https://doi.org/10.1194/jlr.M045930>.
- Nguyen, L.N., Ma, D., Shui, G., Wong, P., Cazenave-Gassiot, A., Zhang, X., Wenk, M.R., Goh, E.L.K., and Silver, D.L. (2014). Mfsd2a is a transporter for the essential omega-3 fatty acid docosahexaenoic acid. *Nature* 509, 503–506. <https://doi.org/10.1038/nature13241>.
- Sugasini, D., Yalagala, P.C.R., Goggin, A., Tai, L.M., and Subbaiah, P.V. (2019). Enrichment of brain docosahexaenoic acid (DHA) is highly dependent upon the molecular carrier of dietary DHA: lysophosphatidylcholine is more efficient than either phosphatidylcholine or triacylglycerol. *J. Nutr. Biochem.* 74, 108231. <https://doi.org/10.1016/j.jnutbio.2019.108231>.
- Tserentsoodol, N., Szein, J., Campos, M., Gordienko, N.V., Fariss, R.N., Lee, J.W., Fliesler, S.J., and Rodriguez, I.R. (2006). Uptake of cholesterol by the retina occurs primarily via a low density lipoprotein receptor-mediated process. *Mol. Vis.* 12, 1306–1318.
- Tserentsoodol, N., Gordienko, N.V., Pascual, I., Lee, J.W., Fliesler, S.J., and Rodriguez, I.R. (2006). Intraretinal lipid transport is dependent on high density lipoprotein-like particles and class B scavenger receptors. *Mol. Vis.* 12, 1319–1333.
- Dornstauder, B., Suh, M., Kuny, S., Gaillard, F., Macdonald, I.M., Clandinin, M.T., and Sauvé, Y. (2012). Dietary docosahexaenoic acid supplementation prevents age-related functional losses and A2E accumulation in the retina. *Invest. Ophthalmol. Vis. Sci.* 53, 2256–2265. <https://doi.org/10.1167/ios.11-8569>.
- Stillwell, W., and Wassall, S.R. (2003). Docosahexaenoic acid: membrane properties of a unique fatty acid. *Chem. Phys. Lipids* 126, 1–27. [https://doi.org/10.1016/s0009-3084\(03\)00101-4](https://doi.org/10.1016/s0009-3084(03)00101-4).
- Cao, D., Kevala, K., Kim, J., Moon, H.S., Jun, S.B., Lovering, D., and Kim, H.Y. (2009). Docosahexaenoic acid promotes hippocampal neuronal development and synaptic function. *J. Neurochem.* 111, 510–521. <https://doi.org/10.1111/j.1471-4159.2009.06335.x>.
- Jun, B., Mukherjee, P.K., Asatryan, A., Kautzmann, M.A., Heap, J., Gordon, W.C., Bhattacharjee, S., Yang, R., Petasis, N.A., and Bazan, N.G. (2017). Elovanoids are novel cell-specific lipid mediators necessary for neuroprotective signaling for photoreceptor cell integrity. *Sci. Rep.* 7, 5279. <https://doi.org/10.1038/s41598-017-05433-7>.
- Adkins, Y., and Kelley, D.S. (2010). Mechanisms underlying the cardioprotective effects of omega-3 polyunsaturated fatty acids. *J. Nutr. Biochem.* 21, 781–792. <https://doi.org/10.1016/j.jnutbio.2009.12.004>.
- Bhatt, D.L., Steg, P.G., Miller, M., Brinton, E.A., Jacobson, T.A., Ketchum, S.B., Doyle, R.T., Jr., Julian, R.A., Jiao, L., Granowitz, C., et al. (2019). REDUCE-IT Investigators. Cardiovascular Risk Reduction with Icosapent Ethyl for Hypertriglyceridemia. *N. Engl. J. Med.* 380, 11–22. <https://doi.org/10.1056/NEJMoa1812792>.
- Nakamura, M.T., Yudell, B.E., and Loor, J.J. (2014). Regulation of energy metabolism by long-chain fatty acids. *Prog. Lipid Res.* 53, 124–144. <https://doi.org/10.1016/j.plipres.2013.12.001>.
- Armento, A., Ueffing, M., and Clark, S.J. (2021). The complement system in age-related macular degeneration. *Cell. Mol. Life Sci.* 78, 4487–4505. <https://doi.org/10.1007/s0018-021-03796-9>.
- Montaigne, D., Butruille, L., and Staels, B. (2021). PPAR control of metabolism and cardiovascular functions. *Nat. Rev. Cardiol.* 18, 809–823. <https://doi.org/10.1038/s41569-021-00569-6>.
- Escandon, P., Vasini, B., Whelchel, A.E., Nicholas, S.E., Matlock, H.G., Ma, J.X., and Karamichos, D. (2021). The role of peroxisome proliferator-activated receptors in healthy and diseased eyes. *Exp. Eye Res.* 208, 108617. <https://doi.org/10.1016/j.exer.2021.108617>.
- Bray, N.L., Pimentel, H., Melsted, P., and Pachter, L. (2016). Near-optimal probabilistic RNA-seq quantification. *Nat. Biotechnol.* 34, 525–527. <https://doi.org/10.1038/nbt.3519>.
- Soneson, C., Love, M.I., and Robinson, M.D. (2015). Differential analyses for RNA-seq: transcript-level estimates improve gene-level

- inferences. *F1000Res.* 4, 1521. <https://doi.org/10.12688/f1000research.7563.2>.
38. Robinson, M.D., McCarthy, D.J., and Smyth, G.K. (2010). edgeR: a Bioconductor package for differential expression analysis of digital gene expression data. *Bioinformatics* 26, 139–140. <https://doi.org/10.1093/bioinformatics/btp616>.
39. Ritchie, M.E., Phipson, B., Wu, D., Hu, Y., Law, C.W., Shi, W., and Smyth, G.K. (2015). limma powers differential expression analyses for RNA-sequencing and microarray studies. *Nucleic Acids Res.* 43, e47. <https://doi.org/10.1093/nar/gkv007>.
40. Raudvere, U., Kolberg, L., Kuzmin, I., Arak, T., Adler, P., Peterson, H., and Vilo, J. (2019). g:Profiler: a web server for functional enrichment analysis and conversions of gene lists (2019 update). *Nucleic Acids Res.* 47, W191–W198. <https://doi.org/10.1093/nar/gkz369>.
41. Luo, W., and Brouwer, C. (2013). Pathview: an R/Bioconductor package for pathway-based data integration and visualization. *Bioinformatics* 29, 1830–1831. <https://doi.org/10.1093/bioinformatics/btt285>.
42. Liberzon, A., Birger, C., Thorvaldsdóttir, H., Ghandi, M., Mesirov, J.P., and Tamayo, P. (2015). The Molecular Signatures Database (MSigDB) hallmark gene set collection. *Cell Syst.* 1, 417–425. <https://doi.org/10.1016/j.cels.2015.12.004>.
43. Yanai, S., and Endo, S. (2021). Functional Aging in Male C57BL/6J Mice Across the Life-Span: A Systematic Behavioral Analysis of Motor, Emotional, and Memory Function to Define an Aging Phenotype. *Front. Aging Neurosci.* 13, 697621. <https://doi.org/10.3389/fnagi.2021.697621>.
44. Nair, A.B., and Jacob, S. (2016). A simple practice guide for dose conversion between animals and human. *J. Basic Clin. Pharm.* 7, 27–31. <https://doi.org/10.4103/0976-0105.177703>.
45. Kuda, O., Brezinova, M., Rombaldova, M., Slavikova, B., Posta, M., Beier, P., Janovska, P., Veleba, J., Kopecky, J., Jr., Kudova, E., et al. (2016). Docosahexaenoic Acid-Derived Fatty Acid Esters of Hydroxy Fatty Acids (FAHFAs) With Anti-inflammatory Properties. *Diabetes* 65, 2580–2590. <https://doi.org/10.2337/db16-0385>.
46. Matthews, D.R., Hosker, J.P., Rudenski, A.S., Naylor, B.A., Treacher, D.F., and Turner, R.C. (1985). Homeostasis model assessment: insulin resistance and beta-cell function from fasting plasma glucose and insulin concentrations in man. *Diabetologia* 28, 412–419. <https://doi.org/10.1007/BF00280883>.
47. Folch, J., Lees, M., and Sloane Stanley, G.H. (1957). A simple method for the isolation and purification of total lipides from animal tissues. *J. Biol. Chem.* 226, 497–509.
48. Patterson, R.E., Ducrocq, A.J., McDougall, D.J., Garrett, T.J., and Yost, R.A. (2015). Comparison of blood plasma sample preparation methods for combined LC-MS lipidomics and metabolomics. *J. Chromatogr. B Anal. Technol. Biomed. Life Sci.* 1002, 260–266. <https://doi.org/10.1016/j.jchromb.2015.08.018>.
49. Lydic, T.A., Busik, J.V., and Reid, G.E. (2014). A monophasic extraction strategy for the simultaneous lipidome analysis of polar and nonpolar retina lipids. *J. Lipid Res.* 55, 1797–1809. <https://doi.org/10.1194/jlr.D050302>.
50. Delektta, P.C., Shook, J.C., Lydic, T.A., Mulks, M.H., and Hammer, N.D. (2018). *Staphylococcus aureus* Utilizes Host-Derived Lipoprotein Particles as Sources of Fatty Acids. *J. Bacteriol.* 200, e007288-17. <https://doi.org/10.1128/JB.00728-17>.
51. Watrous, J.D., Niiranen, T.J., Lagerborg, K.A., Henglin, M., Xu, Y.J., Rong, J., Sharma, S., Vasan, R.S., Larson, M.G., Armando, A., et al. (2019). Directed Non-targeted Mass Spectrometry and Chemical Networking for Discovery of Eicosanoids and Related Oxylipins. *Cell Chem. Biol.* 26, 433–442.e4. <https://doi.org/10.1016/j.chembiol.2018.11.015>.
52. Arunkumar, R., Gorusupudi, A., Li, B., Blount, J.D., Nwagbo, U., Kim, H.J., Sparrow, J.R., and Bernstein, P.S. (2021). Lutein and zeaxanthin reduce A2E and iso-A2E levels and improve visual performance in Abca4-/- Bco2-/- double knockout mice. *Exp. Eye Res.* 209, 108680. <https://doi.org/10.1016/j.exer.2021.108680>.
53. Li, B., Rognon, G.T., Mattinson, T., Vachali, P.P., Gorusupudi, A., Chang, F.Y., Ranganathan, A., Nelson, K., George, E.W., Frederick, J.M., and Bernstein, P.S. (2018). Supplementation with macular carotenoids improves visual performance of transgenic mice. *Arch. Biochem. Biophys.* 649, 22–28. <https://doi.org/10.1016/j.abb.2018.05.003>.
54. Jiang, K., Mondal, A.K., Adlakha, Y.K., Gumerson, J., Aponte, A., Gieser, L., Kim, J.W., Boleda, A., Brooks, M.J., Nellissery, J., et al. (2022). Multiomics analyses reveal early metabolic imbalance and mitochondrial stress in neonatal photoreceptors leading to cell death in Pde6brd1/rd1 mouse model of retinal degeneration. *Hum. Mol. Genet.* 31, 2137–2154. <https://doi.org/10.1093/hmg/ddac013>.
55. Suzuki, T., Ozasa, H., Itoh, Y., Zhan, P., Sawada, H., Mino, K., Walport, L., Ohkubo, R., Kawamura, A., Yonezawa, M., et al. (2013). Identification of the KDM2/7 histone lysine demethylase subfamily inhibitor and its antiproliferative activity. *J. Med. Chem.* 56, 7222–7231. <https://doi.org/10.1021/jm400624b>.

## STAR★METHODS

## KEY RESOURCES TABLE

REAGENT or RESOURCE	SOURCE	IDENTIFIER
<b>Chemicals, peptides, and recombinant proteins</b>		
Sardine Oil	Peru in 2019	N/A
cis-5,8,11,14,17-Eicosapentaenoic acid	Sigma-Aldrich	Cat# E2011
cis-4,7,10,13,16,19-Docosahexaenoic acid	Sigma-Aldrich	Cat# D2534
Isopropanol, Optima LC/MS grade	Fisher Scientific	Cat# A461-4
Methanol, Optima LC-MS grade	Fisher Scientific	Cat# A955-500
Acetonitrile, Optima LC-MS grade	Fisher Scientific	Cat# A955-500
Ethanol, HPLC grade	Fisher Scientific	Cat# AC611050040
Water, Optima LC-MS grade	Fisher Scientific	Cat# W6500
Tert-Butyl Methyl Ether, HPLC Plus grade	Sigma Aldrich	Cat# 650560
Ammonium formate	Alfa Aeser	Cat# 540-69-2
Butylated hydroxytoluene	Sigma Aldrich	Cat# B1378-100G
Acetic Acid, Optima LC/MS grad	Fisher Scientific	Cat# A11350
Phosphatidylcholine (23:0/23:0)	Avanti Polar Lipids	Cat# 850372
Phosphatidylglycerol (14:0/14:0)	Avanti Polar Lipids	Cat# 840445
Phosphatidic acid (14:0/14:0)	Avanti Polar Lipids	Cat# 830845
Phosphatidylethanolamine (14:0/14:0)	Avanti Polar Lipids	Cat# 850745
Phosphatidylserine (14:0/14:0)	Avanti Polar Lipids	Cat# 840033
Sphingomyelin (18:1/12:0)	Avanti Polar Lipids	Cat# 860583
Deuterated (d8)-Arachidonic acid	Cayman Chemical	Cat# 390010
Triglyceride (14:1/14:1/14:1)	NuCheck Prep	Cat# T-205
Liposome kit	Sigma-Aldrich	Cat# L4395-1VL
Oil red O	Poly Scientific, Inc	Cat# S-2146
Hematoxylin and eosin	Leica	Leica
(5Z,8Z,11Z,14Z,17Z)-Icosa-5,8,11,14,17-pentaenoic acid	Combi-Blocks	Cat# QG-5508
LiAlH4	MilliporeSigma	Cat# 199877
Nal	MilliporeSigma	Cat# 383112
Li2CuCl4	MilliporeSigma	Cat# 224308
Jones reagent	MilliporeSigma	Cat# 758035
RNeasy Mini Kit	Qiagen	Cat# 74004
TruSeq Stranded mRNA Sample Prep Kit	Illumina	Cat#: 20020595
Ketamine	Akorn, Inc	Cat# NDC42023-115-10
Xylazine	Akorn, Inc	Cat# NDC59399-110-20
1% tropicamide ophthalmic solution	Akorn, Inc	Cat# NDC17478-102-12
<b>Deposited data</b>		
RNA-seq data	This paper	GEO: GSE221559
<b>Experimental models: Cell lines</b>		
Chinese hamster ovary (CHO) cells	ATCC	CCL-61
<b>Experimental models: Organisms/strains</b>		
Mouse: C57BL/6	Taconic Biosciences	B6NTac

(Continued on next page)

**Continued**

REAGENT or RESOURCE	SOURCE	IDENTIFIER
Mouse: C57BL/6J	Jackson Laboratories	JAX:000664
<b>Oligonucleotides</b>		
Cyp4a10 (Mm02601690_gH)	Life Technologies	Cat# 4331182
Cyp4a14 (Mm00484135_m1)	Life Technologies	Cat# 4331182
Cyp4a31 (Mm07308194_g1)	Life Technologies	Cat# 4351372
Acot1 (Mm01622471_s1)	Life Technologies	Cat# 4331182
Lpl (Mm00434764_m1)	Life Technologies	Cat# 4331182
Pck1 (Mm01247058_m1)	Life Technologies	Cat# 4331182
Pdhb (Mm00499323_m1)	Life Technologies	Cat# 4331182
C9 (Mm00442739_m1)	Life Technologies	Cat# 4331182
C4a (Mm01132415_g1)	Life Technologies	Cat# 4331182
Elov12 (Mm00517086_m1)	Life Technologies	Cat# 4331182
Elov15 (Mm00506717_m)	Life Technologies	Cat# 4331182
Actb (Mm02619580_g1)	Life Technologies	Cat# 4331182
<b>Software and algorithms</b>		
NDP.view2	Hamamatsu Photonics	Cat# U12388-01
Optometry VR, optomotor tests of vision	Cerebral Mechanics Inc.	Cat# Optometry VR 1.7.4
ERG (UTAS visual diagnostic test system)	LKC technologies	Cat# EM for windows version 9.4.0
kallisto	Bray et al. <sup>36</sup>	<a href="https://github.com/pachterlab/kallisto">https://github.com/pachterlab/kallisto</a>
tximport	Soneson et al. <sup>37</sup>	<a href="https://bioconductor.org/packages/release/bioc/html/tximport.html">https://bioconductor.org/packages/release/bioc/html/tximport.html</a>
edgeR	Robinson et al. <sup>38</sup>	<a href="https://bioconductor.org/packages/release/bioc/html/edgeR.html">https://bioconductor.org/packages/release/bioc/html/edgeR.html</a>
limma	Ritchie et al. <sup>39</sup>	<a href="https://bioconductor.org/packages/release/bioc/html/limma.html">https://bioconductor.org/packages/release/bioc/html/limma.html</a>
gProfiler	Raudvere et al. <sup>40</sup>	<a href="https://biit.cs.ut.ee/gprofiler/gost">https://biit.cs.ut.ee/gprofiler/gost</a>
Pathview	Luo et al. <sup>41</sup>	<a href="https://bioconductor.org/packages/release/bioc/html/pathview.html">https://bioconductor.org/packages/release/bioc/html/pathview.html</a>
msigdb	Liberzon et al. <sup>42</sup>	<a href="https://www.gsea-msigdb.org/gsea/msigdb">https://www.gsea-msigdb.org/gsea/msigdb</a>
MGI	Mouse Genome Database	<a href="https://www.informatics.jax.org/">https://www.informatics.jax.org/</a>
tidyverse	R packages	<a href="https://www.tidyverse.org/">https://www.tidyverse.org/</a>
MAVEN metabolomics software v. 2.0.5	Life Technologies	Cat# NC2169324
LIMSA add-in for Microsoft Excel	N/A	<a href="http://www.helsinki.fi/science/lipids/software.html">www.helsinki.fi/science/lipids/software.html</a>
MetaboAnalyst v. 5.0 software	N/A	<a href="http://www.metaboanalyst.ca">www.metaboanalyst.ca</a>
<b>Other</b>		
Cobas® 6000 analyzer	Roche Diagnostics	Cat# ROCHE Cobas 6000
Superose™ 6 10/300 GL column	GE Healthcare	Cat# GE17-5172-01
ÄKTA pure™ chromatography system	GE Healthcare	Cat# 29018224
NanoDrop™ spectrophotometer	Life Technologies	Cat# ND2000CLAPTOP
4200 TapeStation System	Agilent Technologies	Cat# G2991BA
NextSeq 2000	Illumina	Cat# 20038897
Hamamatsu NDP scanner	Hamamatsu Photonics	Cat# RS
Nuclear Magnetic Resonance Spectroscopy (NMR)	Agilent Technologies	Model: Varian INOVA 400
High-Resolution Mass Spectrometry (HRMS)	Waters Corp	Model: Xevo G2-XS QT
ERG instrument (Full field ERG, UTAS E 3000)	LKC technologies	Cat# UTAS E 3000

(Continued on next page)

**Continued**

REAGENT or RESOURCE	SOURCE	IDENTIFIER
OptoMotry	CerebralMechanics Inc.	Optomotry, serial number DP/N 00324H
Fisher Bead Mill 4	Fisher Scientific	Cat# 15-340-164
Ceramic beads	Fisher Scientific	Cat# 15-340-185
Savant Speedvac SC110A	American Laboratory Trading	Cat# 23011
Vortex Genie II	Scientific Industries	Cat# SI-0236
Synergi HydroRP C18AQ 150 × 2 mm, 4 μ, 80A LC-MS column	Phenomenex	Cat# 00F-4375-B0
C18AQ SecurityGuard cartridge	Phenomenex	Cat# AJ0-7510
Shimadzu Prominence HPLC	Prodigy Scientific	Cat# Shimadzu-Prom
Thermo LTQ-Orbitrap Velos mass spectrometer	Labexchange	Cat# 19984
Eppendorf Safe-Lock 2.0 mL tubes, PCR clean	Sigma Aldrich	Cat# EP022363344
Cat# EP022363344	Fisher Scientific	Cat# 06-406-19M
LC-MS vial snap-caps, 11 mm	Fisher Scientific	Cat# 14-823-399
Agilent vial inserts 250 μL	Agilent	Cat# 5183-2085
Bleaching Clay	Mizusawa Industrial Chemicals, Ltd.	Cat# GALLEON EARTH V2
Silica Gel	AGC Si-Tech Co., LTD	Cat# M.S.GEL D-75-60A

**RESOURCE AVAILABILITY****Lead contact**

Further information and requests for resources and reagents should be directed to and will be fulfilled by the lead contact, Alan T. Remaley ([aremaley1@nhlbi.nih.gov](mailto:aremaley1@nhlbi.nih.gov)).

**Materials availability**

There are restrictions to the availability of fish oil-derived VLCPUFA concentrate oil used in the current study, due to external centralized repository for its distribution and our need to maintain the stock.

The chemically synthesized VLCPUFA compounds generated in this study will be made available on request, but we may require a completed materials transfer agreement if there is potential for commercial application.

All other stable reagents generated in this study are available from the [lead contact](#) with a completed materials transfer agreement.

**Data and code availability**

- Data for the key findings of this paper can be downloaded at the NHLBI Figshare website, by searching under the name of the first author of this paper. RNA-seq reads and processed data have been deposited at GEO and are publicly available as of the date of publication. The accession number is listed in the [key resources table](#).
- This paper does not report original code.
- Any additional information required to reanalyze the data reported in this paper is available from the [lead contact](#) upon request.

**EXPERIMENTAL MODEL AND STUDY PARTICIPANT DETAILS**

Black C57BL/6J mice were obtained from Taconic Biosciences (Germantown, NY, USA) and Jackson Laboratories (Bar Harbor, ME, USA). Twenty-four 9-month-old mice, including 12 males and 12 females, were used in a 8-week dietary supplement study. Twenty-five 3-month-old male mice were used in a single-dose gavage study. Sixteen 3-month-old mice, including 8 males and 8 females, were used in a repeated-dose gavage study. All animals, 3–4 mice/cage, housed in a humidity and temperature controlled room (relative humidity, 30–70%; temperature, 20°C–24°C) under a 12/12 light dark cycle with access to food and water *ad libitum*.

**METHOD DETAILS****VLCPUFA concentrate oil derived from fish oil**

VLCPUFA concentrate oil in ethyl ester form enriched in C24–C28 fatty acids was produced from sardine oil. After cholesterol and environmental pollutants, such as dioxins, were removed from oil by short path distillation, ethyl esters were obtained by transesterification with sodium ethoxide, and bleaching of the fish oil was accomplished by treating the oil with bleaching clay. The resulting fish oil ethyl ester was

refined by precision distillation, and fatty acids with carbon chain length less than 20 were removed. The ethyl esters were further purified by thin-film distillation to remove fatty acid ethyl esters with carbon chain length of 22 polymers, and diacylglycerol as much as possible. The ethyl ester oil was further purified by high-performance liquid chromatography with methanol used for the mobile phase. After the final silica gel purification process, peroxides were removed, and VLCPUFA concentrate oil was obtained. The major fatty acid composition is shown in [Table S1](#). VLCPUFAs content was characterized by an Agilent 7890A GC system (Agilent, Palo Alto, CA, USA) coupled with a quadrupole time-of-flight mass spectrometry system (Xevo G2-XS QToF, Waters Corporation, Manchester, U.K.) combined with an atmospheric pressure gas chromatography (APGC) ionization source. The total amount of n-3 VLCPUFAs was 40.4% (w/w), containing 28.5% of 24:5 n-3, 3.3% of 26:6 n-3, and 8.5% of 28:8 n-3, as well as a trace amount of 24:6 n-3 (0.1%).

### Animals experimental design

All experiments were conducted in accordance with guidelines provided by the National Institutes of Health Guide for the Care and Use of Laboratory Animals. The mouse experiments were approved by the Animal Care and Use Committee at the National Heart, Lung and Blood Institute (Protocol Number: H-005-R5/R6) and at the University of Utah (Protocol Number: 00001558). In a dietary supplementation feeding experiment, 9-month-old male and female C57BL/6J mice were fed a chow diet AIN-93G supplemented with 1% or 5% (w/w) VLCPUFA concentrate oil, or none (control) for 8 weeks ( $n = 8$  per group;  $n = 4$  males and  $n = 4$  females per group), in order to evaluate the metabolic effect of dietary VLCPUFAs in early aging normal mice that mimic natural aging process in humans.<sup>43</sup> The 1% and 5% VLCPUFA (w/w) supplementation (40% of purity) are equivalent to approximately 0.67 g/kg and 3.3 g/kg in mice, respectively, which is equivalent to 54 mg/kg and 270 mg/kg in human, respectively, according to an established metabolic body weight formula.<sup>44</sup> The dose and feeding period are comparable with previous animal metabolism studies, using fish oil-derived VLCPUFA concentrate in triglyceride form or dietary DHA.<sup>16,45</sup> Each diet contained equally 18.8% kcal from protein, 63.9% kcal from carbohydrate, and 17.2% kcal from fat. After 8 weeks of diet consumption, the 5-h fasted mice were euthanized via intraperitoneal injection of tribromoethanol. Blood plasma, eye, liver, kidney, spleen, heart, skeleton muscle, small intestine, brain and testis tissues were harvested for the following biochemistry analysis, histology evaluation, lipid extraction and liquid chromatography with tandem mass spectrometry (LC-MS/MS) analysis, or gene expression analysis. In a single-dose gavage experiments, twenty-five 3-month-old male mice were randomized based on age and weight, and they were orally gavage fed with 100  $\mu$ L of VLCPUFA-oil that was prepared with a liposome kit (Millipore Sigma, Burlington, MA, USA). Alpha-tocopherol (0.025%) was added to prevent oxidation of VLCPUFAs. A dose of 6 mg/day/mouse of VLCPUFAs (250 mg/kg body weight) was used. The animals were euthanized at time points of 0, 2, 4, 8, and 24 h ( $n = 5$  per time point). Blood was collected by cardiac puncture into 2 mL heparinized tubes, and blood was centrifuged to 2500 g for 10 min to collect serum. Serum was collected and retinas were dissected from the rest of the eye tissue under a microscope. Lipid was extracted from serum and one pair of retina/mouse for further GC-MS analysis as previously described.<sup>11</sup> In a repeated-dose gavage experiment, 3-month-old male and female mice were randomly divided into the two following treatment groups based on age and weight: VLCPUFA-oil and vehicle (liposome, control) ( $n = 8$  per group;  $n = 4$  males and  $n = 4$  females per group). Vehicle and VLCPUFA-oil (80 mg/kg body weight/day) were administered to the mice by oral gavage once daily for 15 consecutive days. At the end of the experimental period, mice were subjected to ERG and optokinetic response tests. The experimental schemes of the three animal studies are shown in [Figure S1](#). The doses used in the gavage studies were comparable with previous report using chemically synthesized VLCPUFA species.<sup>11</sup>

### Biochemical assays

After 9-month-old mice were fed 0, 1% or 5% VLCPUFA-supplemented diet for 8 weeks, plasma glucose, triglyceride, total cholesterol, phospholipids, bilirubin, chloride, calcium, magnesium, creatinine, aspartate aminotransferase (AST), alanine aminotransferase (ALT), potassium, albumin, total creatine kinase, lactate dehydrogenase, total protein, amylase, inorganic phosphorus, urea nitrogen, and uric acid were measured using routine diagnostic test kits on a Cobas 6000 analyzer (Roche Diagnostics, Indianapolis, IN, USA). Plasma insulin was measured by ELISA according to the manufacturer's directions (R&D Systems, Minneapolis, MN). The HOMA-IR index was calculated according to the formula:  $HOMA-IR = [\text{glucose}] (\text{mmol/L}) \times [\text{insulin}] (\mu\text{U/ml}) / 22.5$  to estimate insulin sensitivity.<sup>46</sup> For FPLC profile analysis, pooled plasma (150  $\mu$ L) from each diet group ( $n = 8$ ) was applied to Superose 6 10/300 GL column on an AKTA-FPLC system (AKTA Pure, GE Healthcare, Chicago, IL, USA). Lipoproteins were eluted with elution buffer, and 0.5 mL fractions were collected at a flow rate of 0.5 mL/min. Total cholesterol and phospholipids levels were measured in FPLC samples according to manufacturer instructions from Fujifilm Wako Chemicals (Richmond, VA, USA). For quantification of hepatic lipid levels, hepatic total lipids were extracted with a mixture of chloroform and methanol (2:1, v/v) as described previously,<sup>47</sup> and the content of TG, phospholipid, and total cholesterol were measured by colorimetric assays (Fujifilm Wako Chemicals).

### Histological analysis

At the end of the 8-week dietary VLCPUFA supplementation period, liver, brain, kidney, spleen, heart, skeletal muscle, small intestine, and testis were embedded in paraffin and sectioned at 5  $\mu$ m, following formalin fixation. All slices were stained with H&E for microscopic examination. Additionally, oil red O stain was performed on fresh frozen liver sections (10  $\mu$ m) to illustrate hepatic lipid accumulation ([Figures S3](#) and [S11](#)). All slides were then scanned with a Hamamatsu NDP scanner (Hamamatsu Photonics, Township, NJ, USA) for histology evaluations by a pathologist in a blinded manner. Semiquantitative scores (0–3) were used to assess histological changes between each diet group: 0: no abnormalities; 1, mild changes; 2, moderate changes and 3, severe changes.

### LC-MS/MS analysis

After mice were fed 0, 1%, or 5% (w/w) VLCPUFA supplemented diet for 8 weeks, lipids from plasma, liver, brain and eyes (one pair of eyes/mouse) ( $n = 8$  per group) were extracted. Briefly, tissues or plasma were combined with  $-20^{\circ}\text{C}$  chilled 75% methanol spiked with a mixture of synthetic lipid and fatty acid internal standards, and homogenized in a bead mill (Fisher Scientific, Hampton, NH, USA). For global lipidomics analysis, 1/3 of the tissue homogenate was subjected to lipid extraction with methyl-tert-butyl-ether according to Patterson et al.<sup>48</sup> The remaining 2/3 of each homogenate was subjected to protein precipitation with ethanol to isolate free fatty acids and metabolites. Characterization of the incorporation of VLCPUFAs into specific tissues was performed by untargeted lipidomic and metabolomic approaches, using Orbitrap HRAM-MS and MS/MS. To determine utilization of VLCPUFAs by incorporation into complex lipids, global untargeted lipidomic analysis was used to identify and quantify individual molecular species of complex lipids including free fatty acids, mono-, di-, and triacylglycerols, free and esterified cholesterol, the phospholipid classes (PC, PE, PG, PI, PA and PS) and their lyso- and ether-linked subclasses, ceramides and other complex sphingolipids including sphingomyelin as previously described.<sup>49,50</sup> LC-MS/MS analysis of free fatty acids and VLCPUFAs was performed according to previous method<sup>51</sup> modified as follows: The analytical column was a Phenomenex Synergi C18AQ 2.0 mm  $\times$  150 mm, 4  $\mu$ m, 80 Å column equipped with a guard cartridge of equivalent chemistry. The flow rate was 200  $\mu\text{L}/\text{min}$ . The gradient was composed of solvents A: (water: acetonitrile 70:30 containing 0.1% acetic acid), B: (acetonitrile:isopropanol 50:50 containing 0.02% acetic acid) and C: (isopropanol containing 0.02% acetic acid). The gradient time program was: from time 0–2 min, 1% B, 0% C. At time of 2.1 min, 50% B, 0% C. From time 2.1–10.0 min, linear gradient from 50% B to 65% B, 0% C. From 10 to 13 min, linear gradient from 65% B, 0% C to 81.7% B, 0% C. From 13 to 16 min, linear gradient from 0% B, 81.7% C to 0% B, 99% C. From 16 to 24 min, hold 0% B, 99% C, then return to starting conditions for 6 min prior to injecting the next sample. For global lipidomics and free fatty acid analysis, a Thermo Fisher Scientific LTQ-Orbitrap Velos mass spectrometer was used as the detector. Multivariate data analyses using partial least squares-discriminant analysis (PLS-DA) and heatmap generation were performed using MetaboAnalyst 5.0 software ([www.metaboanalyst.ca](http://www.metaboanalyst.ca)).

### ERG and visual behavior testing

ERG and visual behavior exam were used to assess the retinal function of mice after 15 consecutive days of oral gavage of VLCPUFA-oil as described previously.<sup>52</sup> Briefly, mice were dark adapted overnight prior to ERG recording, and procedures were conducted in a lightproof room with the aid of a dim red light. Upon induction of anesthesia by i.p. injection of 80 mg/kg Ketamine +10 mg/kg xylazine and mydriasis (1% tropicamide ophthalmic solution), mice were placed on a thermostatically controlled heating pad, and a gold corneal and a stainless-steel scalp electrode were used to measure ERG using a UTAS E-3000 (LKC Technologies, Gaithersburg, MD). Stimulus response functions were obtained under dark- and then light-adapted conditions, and ERG a-wave and b-wave amplitudes in multiple flash luminances were measured and analyzed. In addition, the optokinetic behavioral tests were performed to analyze the visual function of mice. Visual acuity and contrast sensitivity were measured using an optokinetic testing system (OptoMotry, CerebralMechanics Inc, Medicine Hat, Alberta, Canada), a validated noninvasive methodology previously reported.<sup>53</sup> In brief, the tracking response (optokinetic reflex) was recorded to a rotating visual stimulus displayed on LCD panels surrounding the mouse. Visual acuity was measured at 100% contrast and 12°/s rotation speed, and the contrast sensitivity was measured at spatial frequencies at 0.19 cycles/degree. All the experiments had concurrent age-matched control mice fed with liposomes (control).

### RNA-sequencing analysis

After mice had been fed a chow diet supplemented with 0, 1, or 5% VLCPUFAs for 8 weeks, total RNA was isolated from liver samples ( $n = 6$ /group) using a RNeasy Mini Kit (Qiagen, Hilden, Germany) according to the manufacturer's instructions. RNA purity and concentration were assessed using a NanoDrop spectrophotometer (Thermo Fisher Scientific Inc., Waltham, MA, USA). A 4200 TapeStation System (Agilent Technologies, Santa Clara, CA, USA) was used with RNA screentapes to generate RNA integrity numbers (RIN) for RNA samples. All RNA samples selected for RNA-seq library preparation had a RIN greater than 7. RNA-seq libraries were prepared using a TruSeq Stranded mRNA Sample Prep Kit (Illumina, San Diego, CA, USA). RNA seq data was handled as described previously.<sup>54</sup> Briefly, 125-bp paired reads were generated using Illumina Nextseq. Post quality check, reads were mapped to the reference transcriptome using kallisto<sup>36</sup> alignments were imported into R and processed with tximport<sup>37</sup> and the Mus musculus Ensembl annotation (GRCm39 v104) to summarize gene counts. Lowly expressing genes were filtered out by only retaining genes that had greater than 3 CPM expression in two or more samples. Differential expression analysis was performed with the edgeR<sup>38</sup> and limma-voom pipeline,<sup>39</sup> and thresholds of 0.1 FDR and 1.5-fold change ( $\text{abs}(\log 2\text{FC}) > 0.58$ ) were used to determine significant differentially expressed genes. The gene expression data generated from RNA-seq analysis have been deposited in the NCBI's Gene Expression Omnibus (GEO) database (GEO: GSE221559). The gProfiler API<sup>40</sup> was utilized for pathway enrichment, followed by visualization using custom scripts or the pathview R package.<sup>41</sup> Pathway annotation for targeted analyses were obtained from gProfiler, msigdb<sup>42</sup> and MGI. Unless otherwise mentioned, all other analyses were performed using base R packages and the tidyverse library.

### Quantitative PCR (qPCR) validation

One  $\mu\text{g}$  of total RNA was reverse transcribed to cDNA using a QuantiNova Reverse Transcription Kit (QIAGEN Sciences Inc., Germantown, MD, USA), and real-time PCR reactions were conducted on a QuantStudio 5 Real-Time PCR system (Applied Biosystems, Waltham, MA, USA)

using TaqMan probes ( $n = 8/\text{group}$ ). The following primer probes (Thermo Fisher Scientific, Waltham, MA) were used: *Cyp4a10*, *Cyp4a14*, *Cyp4a31*, *Acot1*, *Lpl*, *Pck1*, *Pdhb*, *C9*, *C4a*, *Elovl2*, *Elovl5*. The housekeeping gene  $\beta$ -actin was used as the reference gene.

### Chemical synthesis of 24:5 n-3

(5Z,8Z,11Z,14Z,17Z)-Icosa-5,8,11,14,17-pentaenoic acid with 97% of purity (Combi-Blocks, Inc., San Diego, CA) was reduced with LiAlH<sub>4</sub> to pentaen-1-ol in 92% yield, followed by conversion to tosylate and then iodide in 77% yield in a two-step reaction. The key coupling reaction was performed with iodide and a Li<sub>2</sub>CuCl<sub>4</sub> catalyzed Grignard reaction with (4-((tetrahydro-2H-pyran-2-yl)oxy)butyl)magnesium bromide at  $-10^{\circ}\text{C}$  to produce 2-(((9Z,12Z,15Z,18Z,21Z)-tetracosa-9,12,15,18,21-pentaen-1-yl)oxy)tetrahydro-2H-pyran in 89% yield.<sup>55</sup> After deprotection of -OTHP group followed by Jones oxidation, the final product 24:5 n-3 with >99% of purity was obtained. The structure and purity of 24:5 n-3 were determined by <sup>1</sup>H NMR, <sup>13</sup>C NMR and high-resolution mass spectrometry (HRMS) (Figure S2). <sup>1</sup>H NMR (400 MHz, CDCl<sub>3</sub>):  $\delta$  5.41–5.32 (m, 10H, =C-H), 2.86–2.80 (m, 8H, =-CH<sub>2</sub>-), 2.35 (t,  $J = 7.6\text{ Hz}$ , 2H, -CH<sub>2</sub>-CO<sub>2</sub>), 2.10–2.06 (m, 4H, =-CH<sub>2</sub>-), 1.64 (m, 2H, CH<sub>2</sub>-C-CO<sub>2</sub>), 1.40–1.31 (m, 10H, -(CH<sub>2</sub>)<sub>4</sub>-), 0.98 (t,  $J = 7.4\text{ Hz}$ , 3H, -CH<sub>3</sub>). <sup>13</sup>C NMR (100 MHz, CDCl<sub>3</sub>):  $\delta$  178.57, 132.01, 130.29, 128.53, 128.49, 128.16, 127.90, 127.88, 127.65, 127.00, 33.75, 29.54, 29.12, 29.05, 29.00, 27.19, 25.62, 25.52, 24.65, 20.53, 14.23. HRMS: calculated for C<sub>24</sub>H<sub>39</sub>O<sub>2</sub> [M + H] 359.2950, observed 359.2947.

### In vitro PPARs agonist activity assay

The human peroxisome proliferator-activated receptors (PPARs) agonist activity assay was performed using PPAR- $\alpha$  or PPAR $\gamma$ -luciferase reporter assay kits (Indigo Biosciences, State College, PA) according to the manufacturer's instructions. Briefly, Chinese Hamster Ovary (CHO) cells that have a luciferase reporter gene functionally linked to a PPAR $\alpha$  or PPAR $\gamma$ -response element were used to quantify changes in luciferase expression, a surrogate measure of the changes in PPAR activity. Reporter cells seeded in 96-well plates were treated with fish oil-derived VLCPUFA-oil, chemically synthesized 24:5 n-3, or purified EPA or DHA (Sigma Aldrich, St. Louis, MO, USA) that were dissolved in ethanol for approximately 24 h before luciferase activity assay using Luminoskan Ascent Microplate Luminometer (Thermo Fisher Scientific). All measurements were performed in triplicate. Ethanol in PBS was used as a vehicle control.

### QUANTIFICATION AND STATISTICAL ANALYSIS

Statistical analyses were performed using GraphPad Prism statistical software (GraphPad Software, USA, version 6.). A one-way ANOVA with Tukey's post hoc test for multiple comparisons was used to compare the difference among multiple groups, and a two-tailed Student's t-test was used for the comparison between two groups. Results are presented as means  $\pm$  SEM, and the significance level was set at 0.05.